



Published in final edited form as:

*J Am Chem Soc.* 2016 August 31; 138(34): 10766–10769. doi:10.1021/jacs.6b06177.

## Impact of $\gamma$ -Amino Acid Residue Preorganization on $\alpha/\gamma$ -Peptide Foldamer Helicity in Aqueous Solution

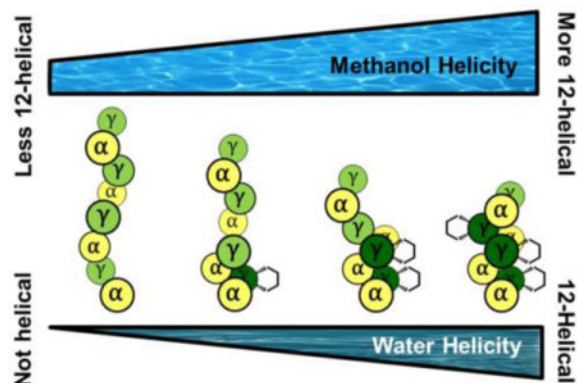
Brian F. Fisher and Samuel H. Gellman\*

Department of Chemistry, University of Wisconsin-Madison, Madison, Wisconsin 53706, United States

### Abstract

$\alpha/\gamma$ -Peptide foldamers containing either  $\gamma^4$ -amino acid residues or ring-constrained  $\gamma$ -amino acid residues have been reported to adopt 12-helical secondary structure in nonpolar solvents and in the solid state. These observations have engendered speculation that the seemingly flexible  $\gamma^4$  residues have a high intrinsic helical propensity, and that residue-based preorganization may not significantly stabilize the 12-helical conformation. However, the prior studies were conducted in environments that favor intramolecular H-bond formation. In this report, we use 2D-NMR to compare the ability of  $\gamma^4$  residues and cyclic  $\gamma$  residues to support 12-helix formation in more challenging environments, methanol and water. Both  $\gamma$  residue types support 12-helical folding in methanol, but only the cyclically constrained  $\gamma$  residues promote helicity in water. These results demonstrate the importance of residue-based preorganization strategies for achieving stable folding among short foldamers in aqueous solution.

### TOC image



Corresponding Author: gellman@chem.wisc.edu.

Supporting Information

Experimental details, including synthetic route to **II**; NMR spectra; HDX, VT-NMR, and *J*-coupling analysis; ROESY crosspeak assignments; CD data; comparison of **I** and  $\gamma^4$  structure; and NMR calculation parameters. This material is available free of charge via the Internet at <http://pubs.acs.org>.

Notes

The authors declare no competing financial interest.

The study of unnatural oligomers that display biopolymer-like folding behavior offers a framework for interrogating relationships between covalent and noncovalent structure (constitution and conformation) in a way that transcends the deep understanding that has emerged from analysis of proteins and nucleic acids. For example, examination of “foldamers” that contain  $\beta$ -amino acid residues instead of or in addition to  $\alpha$  residues (i.e.,  $\beta$ -peptides or  $\alpha/\beta$ -peptides) has revealed the strong influence of small-ring constraints on the identity and stability of H-bond-mediated secondary structure.<sup>1</sup> This issue is not pertinent to the folding of conventional polypeptides, containing exclusively  $\alpha$  residues, because imposition of a cyclic constraint necessarily abolishes backbone H-bond potential and disrupts common secondary structures, as seen with proline residues.<sup>2</sup>

Insights gained from experimental correlations among residue identity, secondary structure and conformational stability have proven invaluable in the development of functional foldamers containing  $\beta$  residues. Stabilization of the  $\beta$ -peptide 14-helix by *trans*-cyclohexyl residues, for example, enabled development of a foldamer catalyst<sup>3</sup> and fundamental single-molecule studies of hydrophobic interactions.<sup>4</sup> Stabilization of  $\alpha/\beta$ -peptide helices by *trans*-cyclopentyl residues has allowed the refinement of protein-protein interaction antagonists.<sup>5</sup> These functional outcomes with  $\beta$ -containing foldamers highlights the importance of elucidating relationships between residue structure and conformational stability to other foldamer classes. Here we evaluate the impact of a specific cyclic constraint on helical secondary structure formed by  $\alpha/\gamma$ -peptides.

Peptidic foldamers containing  $\gamma$  residues have been examined in many laboratories,<sup>6</sup> but only a few studies<sup>7</sup> have evaluated the relationships between  $\gamma$  residue structure and conformational stability. The  $\alpha/\gamma$ -peptide 12-helix is probably the most extensively studied secondary structure in this foldamer class. This conformation, formed by oligomers with sequentially alternating  $\alpha$  and  $\gamma$  residues, is defined by 12-atom  $C=O(i) \rightarrow H-N(i+3)$  H-bonds between backbone amide groups. The  $\alpha/\gamma$ -peptide 12-helix was initially observed by Balaram and coworkers in crystal structures of achiral oligomers containing gabapentin (Gpn) and  $\alpha$ -aminoisobutyric acid (Aib) residues.<sup>8,9</sup> Guo *et al.* developed an efficient asymmetric synthesis leading to trisubstituted  $\gamma$ -amino acid residue **I** (Figure 1), and showed that  $\alpha/\gamma$ -peptides containing **I** form the 12-helix in chloroform (based on NOE analysis) and in the crystalline state.<sup>10</sup> The cyclic constraint and substitution pattern of **I** should limit conformational freedom. In particular, the  $C\alpha-C\beta$  and  $C\beta-C\gamma$  bonds are predicted to favor a  $g^+,g^+$  torsion angle sequence, as required for the 12-helix; this prediction is consistent with the many crystal structures of foldamers containing residue **I**.<sup>11</sup>

The groups of Gopi<sup>12</sup> and Balaram<sup>13</sup> have reported a large set of crystal structures showing that  $\alpha/\gamma$ -peptides containing exclusively  $\gamma^4$  residues (Figure 1) (4-mers to 16-mers) can adopt the 12-helix. In these structures the  $C\alpha-C\beta$  and  $C\beta-C\gamma$  torsion angles favor a  $g^+,g^+$  torsion sequence similar to that observed in 12-helices containing residue **I**. Balaram and coworkers further demonstrated via 2D NMR that 12-helicity is maintained by a 16-mer  $\alpha/\gamma$ -peptide in chloroform.<sup>13b</sup> These findings are striking because one would predict  $\gamma^4$  residues to be much more flexible than is  $\gamma$  residue **I**. As Balaram and coworkers noted, the extensive structural results with  $\alpha/\gamma^4$ -peptides lead one to question whether the constraint inherent in **I** stabilizes the 12-helical conformation. This uncertainty must be resolved

because constrained residues generally require greater synthetic effort than do flexible residues.

To address this question, we moved to a new family of  $\alpha/\gamma$ -peptide octamers (**1-4**; Figure 2) tailored for aqueous solubility. Water is the least favorable among common solvents for H-bonded conformations such as the  $\alpha$ -helix or  $\beta$ -sheets formed by conventional peptides or helices formed by  $\beta$ - or  $\alpha/\beta$ -peptide foldamers.<sup>14</sup> Presumably the strong H-bond competition provided by water molecules diminishes the ability of intramolecular H-bonds to stabilize secondary structure. Admixture of an alcohol cosolvent, such as methanol, enhances the population of internally H-bonded secondary structures for which there is an intrinsic propensity,<sup>14-15</sup> but aqueous-alcohol mixtures do not guarantee folding. In contrast, chloroform allows intramolecular H-bonds to serve as a strong driving force for secondary structure formation. Qualitative comparisons based on data obtained in chloroform or crystal structures cannot decisively address the relative 12-helical propensities of **I** vs. a  $\gamma^4$  residue.

$\alpha/\gamma$ -Peptide series **1-4** features both  $\gamma^4$  residues and  $\gamma$  residue **II** (Figure 1), which is an analogue of **I** bearing a side chain that should be cationic at acidic pH.  $\alpha/\gamma$ -Peptide **1** contains exclusively  $\gamma^4$  residues, which are progressively replaced with **II**, from N- to C-terminus, in analogues **2-4**. The  $\gamma$  residue side chain complement varies at one position across the  $\alpha/\gamma$ -peptide series: **1** and **2** have a glutamate-like side chain at residue 4, but **3** and **4** have a lysine-like side chain at this position. This variation was intended to promote <sup>1</sup>H NMR resonance dispersion. The four  $\alpha$  residues are invariant among **1-4**. Two aromatic side chains (Tyr-5 and Phe-7) were included to enhance dispersion of <sup>1</sup>H NMR signals.

Initial 2D NMR studies were conducted in CD<sub>3</sub>OH, in which **1-4** were highly soluble. <sup>1</sup>H resonances were unchanged between 0.1 and 3 mM, suggesting that aggregation state, which we assume to be monomeric, does not vary in this range. In general, more constrained  $\gamma$  residues correlated with improved chemical shift dispersion. In order to detect 12-helical folding, we focused on three types of backbone-to-backbone *i,i+2* NOE that are known to be characteristic of this secondary structure (Table 1).<sup>10, 13b</sup>

For fully flexible  $\alpha/\gamma$ -peptide **1** in CD<sub>3</sub>OH, partial chemical shift overlap precluded precise integration of several expected 12-helical crosspeaks in the 2D-ROESY spectrum. Nevertheless, unambiguous observation of six characteristic NOEs, uniformly distributed across **1**, supported the conclusion that this  $\alpha/\gamma$ -peptide is at least partially 12-helical in methanol (Table 1).

Improved <sup>1</sup>H signal dispersion enabled unambiguous assignment of almost all expected 12-helix NOEs for  $\alpha/\gamma$ -peptide **2** in CD<sub>3</sub>OH. The two 12-helical NOEs involving the cyclic  $\gamma$  residue (types **a** and **b** in Table 1) were more intense than those involving  $\gamma^4$  residues. The 12-helical NOEs involving the  $\alpha$  residues (type **c**) were generally not very intense; consistent with this trend, protons that would give rise to type **c** NOEs are further apart in available 12-helix crystal structures than are protons that would give rise to type **a** or **b** NOEs.<sup>12c</sup>  $\alpha/\gamma$ -Peptide **3**, containing two cyclic  $\gamma$  residues, showed excellent chemical shift dispersion, and numerous 12-helical NOEs were detected. As seen for **2**, crosspeak intensity

was lower for  $\gamma$ -to- $\gamma$  NOEs involving exclusively  $\gamma^4$  residues relative to such NOEs involving at least one cyclic  $\gamma$  residue.

$\alpha/\gamma$ -Peptide **4**, containing three cyclic  $\gamma$  residues, showed the most intense 12-helical crosspeaks among the four oligomers. Furthermore, numerous long-range NOEs between protons on side chains were detected that were not observed for **1-3**. Collectively, the ROESY spectra for **1-4** in CD<sub>3</sub>OH demonstrate a tendency of all  $\alpha/\gamma$ -peptides to adopt the 12-helix conformation, but the trend of increasing crosspeak intensity and number with increasing number of  $\gamma^4 \rightarrow \mathbf{II}$  replacements suggests that the helical state becomes more stable as cyclic constraints are added.

We next characterized the folding behavior of  $\alpha/\gamma$ -peptides **1-4** in water. All four  $\alpha/\gamma$ -peptides were highly soluble (>3 mM), and chemical shifts did not vary between 0.1 and 3 mM. The data obtained in this competitive environment support our conclusion that the cyclic constraint of residue **II** stabilizes the 12-helix.

For the fully flexible  $\alpha/\gamma$ -peptide **1**, only two very weak  $i,i+2$  ROESY crosspeaks consistent with the 12-helix conformation could be distinguished, with most others impossible to assign unambiguously because of poor resonance dispersion. For all ambiguous  $i,i+2$  crosspeaks, the low intensity outside the overlapping region means that, at most, these NOEs are very weak. Three of the anticipated 12-helical  $i,i+2$  crosspeaks would have occurred in relatively uncrowded regions of the 2D-ROESY spectrum but were not detected, which suggests that any tendency toward 12-helical folding by  $\alpha/\gamma$ -peptide **1** is low in water. Three of the five non-sequential crosspeaks that could be unambiguously assigned were inconsistent with the 12-helix conformation (Figure 3). The  $i,i+2$  NOEs of **1** in water fail to converge to a single mean structure and thus reflect a disordered conformational ensemble.<sup>16</sup>

The aqueous 2D-ROESY spectra of  $\alpha/\gamma$ -peptides **2-4** traced the formation of helicity with increasing cyclic constraint content. As seen in CD<sub>3</sub>OH, the <sup>1</sup>H resonances become more dispersed with increasing content of cyclic  $\gamma$  residue **II**, permitting unambiguous detection of an increasing fraction of the expected 12-helical ROESY crosspeaks as the content of **II** grows. All observed  $i,i+2$  ROESY crosspeaks for **2-4** involve at least one residue **II** or occur between protons from  $\alpha$  residues that are separated by a residue **II**.  $\alpha/\gamma$ -Peptide **2**, with a single residue **II**, illustrates the difference between cyclic and acyclic  $\gamma$  residues in terms of supporting local folding (Figure 4). The crosspeak of type **a** between **II**-2 and  $\gamma^4$ Glu-4 is very intense, whereas the possible **a** crosspeak between  $\gamma^4$ Glu-4 and  $\gamma^4$ Lys-6 is not detected, even though this crosspeak would have occurred in an uncrowded region of the 2D spectrum. This trend continues for  $\alpha/\gamma$ -peptides **3** and **4**.

Results of NOE distance-restrained simulated annealing calculations<sup>17</sup> suggest an increasingly well-defined helical conformation in methanol as  $\gamma^4$  residues are replaced with constrained residues (Figure 5a). The calculations in water suggest an even more pronounced disorder-to-order transition across the series **1-4** than is evident in methanol (Figure 5b vs. Figure 5a). The non-12-helical NOEs of **1** in water result in a variety of simulated conformations that do not correspond to a regular helix. For  $\alpha/\gamma$ -peptides **2** and **3** in water, partial ordering only at the segments containing cyclic  $\gamma$  residues is observed,

which is expected since there was a consistent lack of characteristic  $i,i+2$  ROESY crosspeaks for the segments containing  $\gamma^4$  residues.  $\alpha/\gamma$ -Peptide **4** in water displays a relatively tight cluster of structures, each with the maximum number of 12-helix H-bonds. Increasing the number of  $\gamma^4 \rightarrow \mathbf{II}$  replacements across the series **1-4** improves the overlay of the NMR-derived structures with 12-helical conformations observed for crystalline  $\alpha/\gamma$ -peptides, whether the oligomer crystallized contains constrained  $\gamma$  residue **I** or unconstrained  $\gamma^4$  residues; this trend is illustrated for a specific  $\alpha/\gamma^4$ -peptide crystal structure in Figure 6.

The 2D-NMR data presented here for  $\alpha/\gamma$ -peptides **1-4**, as well as other  $^1\text{H}$ -NMR data,<sup>18</sup> support the hypothesis that the cyclic constraint in **II** stabilizes the 12-helix.  $\gamma^4$  Residues, intrinsically more flexible than is **II**, have a modest propensity for 12-helix formation, as indicated by previous reports<sup>12-13</sup> and by our NMR results in methanol. However, analysis of **1-4** in aqueous solution reveals a clear distinction between 12-helical propensities of **II** and  $\gamma^4$  residues, which decisively addresses questions raised by recent studies.<sup>12-13</sup> These results are significant since the impact of  $\gamma$  residue constraint on foldamer secondary structure has received very little scrutiny, in part because there has been very little previous study of  $\gamma$ -containing foldamers in aqueous solution.<sup>11c, 19</sup> Our demonstration that the preorganization inherent in  $\gamma$  residue **II** favors a specific secondary structure should encourage fundamental research on new foldamer building blocks that favor adoption of discrete and diverse conformations.

## Supplementary Material

Refer to Web version on PubMed Central for supplementary material.

## Acknowledgments

This work was supported by NSF grant CHE-1307365. NMR spectrometers were purchased with support from a generous gift by Paul J. Bender and from NIH (S10 OD012245).

## References

1. (a) Appella DH, Christianson LA, Karle IL, Powell DR, Gellman SH. *J Am Chem Soc.* 1996; 118:13071. (b) Appella DH, Christianson LA, Klein DA, Powell DR, Huang X, Barchi JJ Jr, Gellman SH. *Nature.* 1997; 387:381. [PubMed: 9163422] (c) Hayen A, Schmitt MA, Ngassa FN, Thomasson KA, Gellman SH. *Angew Chem Int Ed.* 2004; 43:505. (d) De Pol S, Zorn C, Klein CD, Zerbe O, Reiser O. *Angew Chem Int Ed.* 2004; 43:511. (e) Fernandes C, Faure S, Pereira E, Théry V, Declerck V, Guillot R, Aitken DJ. *Org Lett.* 2010; 12:3606. [PubMed: 20704401] (f) Lee M, Shim J, Kang P, Choi MG, Choi SH. *Chem Commun.* 2016; 52:5950.
2. (a) O'Neil KT, DeGrado WF. *Science.* 1990; 250:646. [PubMed: 2237415] (b) Minor DL Jr, Kim PS. *Nature.* 1994; 367:660. [PubMed: 8107853]
3. Müller MM, Windsor MA, Pomerantz WC, Gellman SH, Hilvert D. *Angew Chem Int Ed.* 2009; 48:922.
4. Ma CD, Wang C, Acevedo-Vélez C, Gellman SH, Abbott NL. *Nature.* 2015; 517:347. [PubMed: 25592540]
5. Johnson LM, Gellman SH. *Methods Enzymol.* 2013; 523:407. [PubMed: 23422441]
6. (a) Hanessian S, Luo X, Schaum R, Michnick S. *J Am Chem Soc.* 1998; 120:8569. (b) Seebach D, Brenner M, Rueping M, Schweizer B, Jaun B. *Chem Commun.* 2001:207. (c) Bouillère F, Thétiot-Laurent S, Kouklovsky C, Alezra V. *Amino Acids.* 2011; 41:687. [PubMed: 21455734] (d) Nodes

- WJ, Nutt DR, Chippindale AM, Cobb AJA. *J Am Chem Soc.* 2009; 131:16016. [PubMed: 19827809] (e) Pendem N, Nelli YR, Douat C, Fischer L, Laguerre M, Ennifar E, Kauffmann B, Guichard G. *Angew Chem Int Ed.* 2013; 52:4147.(f) Mathieu L, Legrand B, Deng C, Vezenkov L, Wenger E, Didierjean C, Amblard M, Averlant-Petit MC, Masurier N, Lisowski V, Martinez J, Maillard LT. *Angew Chem Int Ed.* 2013; 52:6006.
7. (a) Grison CM, Robin S, Aitken DJ. *Chem Commun.* 2015; 51:16233.(b) Grison CM, Robin S, Aitken DJ. *Chem Commun.* 2016; 52:7802.
8. (a) Ananda K, Vasudev PG, Sengupta A, Raja KM, Shamala N, Balaram P. *J Am Chem Soc.* 2005; 127:16668. [PubMed: 16305256] (b) Vasudev PG, Ananda K, Chatterjee S, Aravinda S, Shamala N, Balaram P. *J Am Chem Soc.* 2007; 129:4039. [PubMed: 17348653]
9. Vasudev PG, Chatterjee S, Shamala N, Balaram P. *Acc Chem Res.* 2009; 42:1628. [PubMed: 19572698]
10. Guo L, Chi Y, Almeida AM, Guzei IA, Parker BK, Gellman SH. *J Am Chem Soc.* 2009; 131:16018. [PubMed: 19886693]
11. (a) Guo L, Almeida AM, Zhang W, Reidenbach AG, Choi SH, Guzei IA, Gellman SH. *J Am Chem Soc.* 2010; 132:7868. [PubMed: 20491510] (b) Guo L, Zhang W, Reidenbach AG, Giuliano MW, Guzei IA, Spencer LC, Gellman SH. *Angew Chem Int Ed.* 2011; 50:5843.(c) Shin YH, Mortenson DE, Satyshur KA, Forest KT, Gellman SH. *J Am Chem Soc.* 2013; 135:8149. [PubMed: 23701135]
12. (a) Bandyopadhyay A, Gopi HN. *Org Lett.* 2012; 14:2770. [PubMed: 22594343] (b) Bandyopadhyay A, Jadhav SV, Gopi HN. *Chem Commun.* 2012; 48:7170.(c) Jadhav SV, Bandyopadhyay A, Gopi HN. *Org Biomol Chem.* 2013; 11:509. [PubMed: 23212647] (d) Jadhav SV, Misra R, Singh SK, Gopi HN. *Chem Eur J.* 2013; 19:16256. [PubMed: 24151124] (e) Jadhav SV, Misra R, Gopi HN. *Chem Eur J.* 2014; 20:16523. [PubMed: 25346477]
13. (a) Basuroy K, Dinesh B, Shamala N, Balaram P. *Angew Chem Int Ed.* 2012; 51:8736.(b) Sonti R, Dinesh B, Basuroy K, Raghothama S, Shamala N, Balaram P. *Org Lett.* 2014; 16:1656. [PubMed: 24588077]
14. (a) Appella DH, Barchi JJ, Durell SR, Gellman SH. *J Am Chem Soc.* 1999; 121:2309.(b) LePlae PR, Fisk JD, Porter EA, Weisblum B, Gellman SH. *J Am Chem Soc.* 2002; 124:6820. [PubMed: 12059191] (c) Vaz E, Pomerantz WC, Geyer M, Gellman SH, Brunsveld L. *ChemBioChem.* 2008; 9:2254. [PubMed: 18756554] (d) Schmitt MA, Choi SH, Guzei IA, Gellman SH. *J Am Chem Soc.* 2005; 127:13130. [PubMed: 16173725]
15. Arvinte T, Drake AF. *J Biol Chem.* 1993; 268:6408. [PubMed: 8454613]
16. Zagrovic B, van Gunsteren WF. *Proteins.* 2006; 63:210. [PubMed: 16425239]
17. Brunger AT. *Nat Protoc.* 2007; 2:2728. [PubMed: 18007608]
18. See Supporting Information for discussion.
19. Sawada T, Gellman SH. *J Am Chem Soc.* 2011; 133:7336. [PubMed: 21520956]

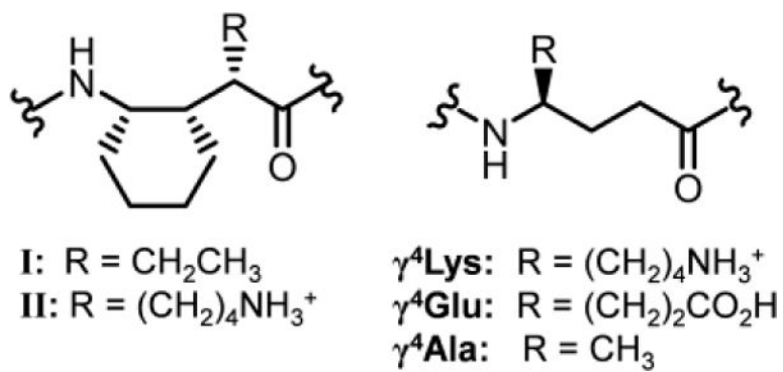


**Figure 1.**  
Structures of  $\gamma$  residues.

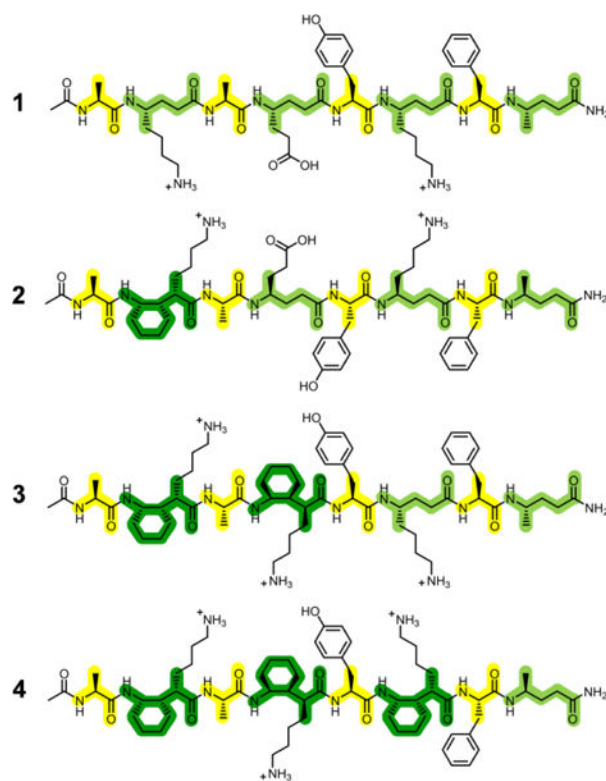


**Figure 2.**  
Structures of water-soluble  $\alpha/\gamma$ -peptides.



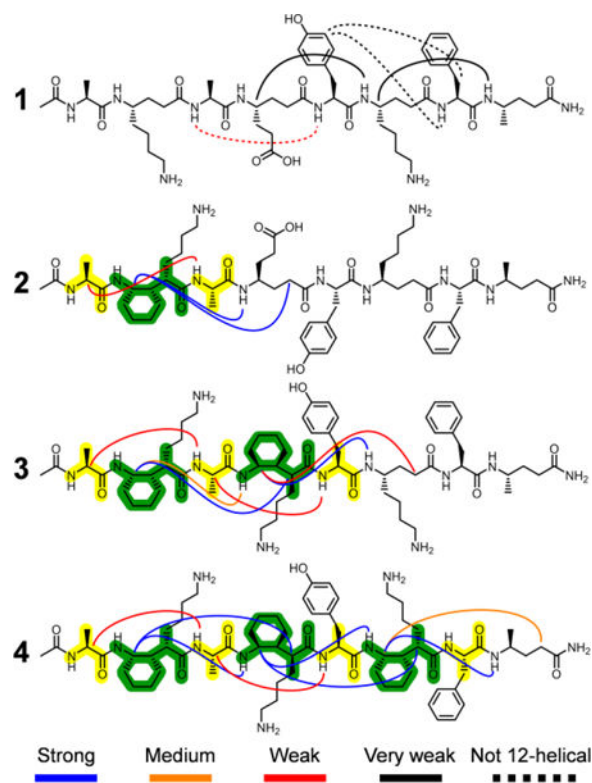


**Figure 3.**  
Summary of detected ROESY crosspeaks between protons on non-adjacent residues in aqueous solution.

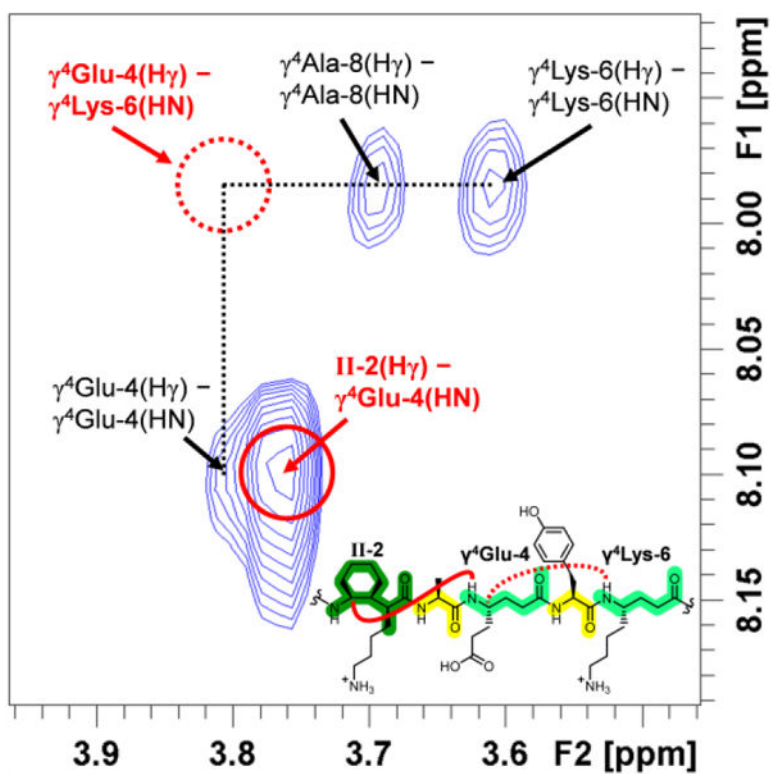


**Figure 4.** Excerpt of the 600 MHz ROESY spectrum of 3 mM  $\alpha/\gamma$ -peptide **2** in 9:1 H<sub>2</sub>O:D<sub>2</sub>O, 100 mM acetate, pH 3.8 at 5°C.  $i, i+2$  NOEs indicated in red. Missing type a NOE shown with dashed line; observed a NOE shown with unbroken line.

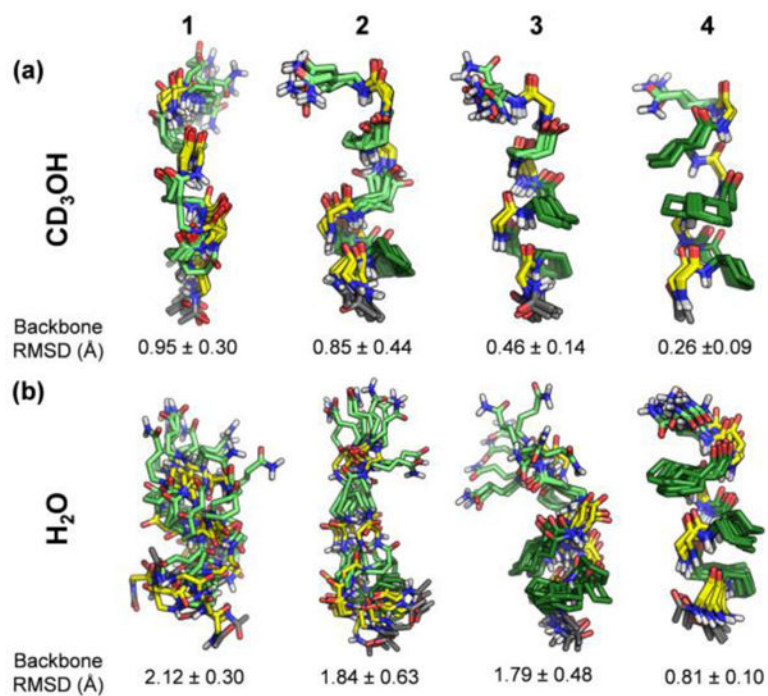


**Figure 5.** Superposition of ten lowest-energy of 100 trial structures from simulated annealing calculations of **1-4**. Mean pairwise backbone RMSD is shown below each structure. (a) Calculated ensembles using distance restraints derived from  $\text{CD}_3\text{OH}$  ROESY data. (b) Calculated ensembles using distance restraints derived from aqueous ROESY data.

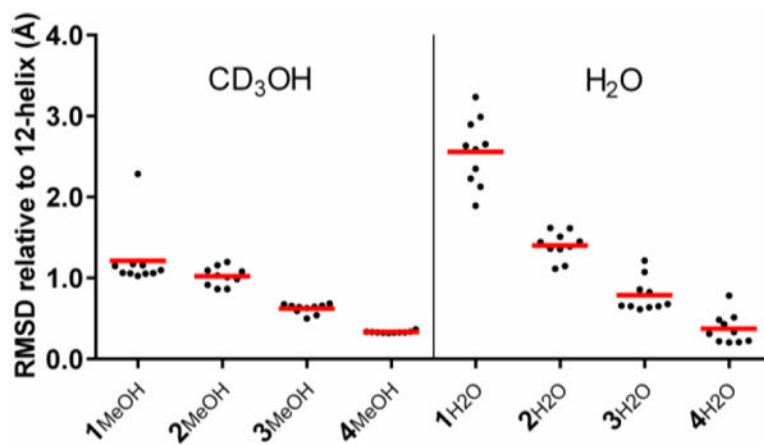
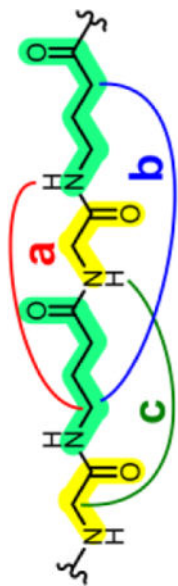


**Figure 6.** Comparison of NMR structures of  $\alpha/\gamma$ -peptides **1-4** with a 12-helix crystal structure from ref. 11c. Black dots are backbone RMSDs of the 10 lowest-energy NMR structures. Mean pairwise RMSDs of each set of NMR structures vs. the crystal structure are shown with red bars.

Table 1

Summary of crosspeaks observed in CD<sub>3</sub>OH.<sup>a</sup>



H atom pair	12-Helix distance (Å) <sup>b</sup>	NOE pairs	1	2	3	4
<b>a</b>	2.72	2 ...4	W	S	?	S
	2.70	4 ...6	?	M	S	S
	2.37	6 ...8	S	M	M	M
<b>b</b>	2.60 <sup>c</sup>	2 ...4	W	S	S	?
	2.69 <sup>c</sup>	4 ...6	?	W	M	S
	–	6 ...8	?	?	W	S
<b>c</b>	3.42	1 ...3	W	W	W	W
	3.64	3 ...5	VW	N.D.	W	W
	3.40	5 ...7	VW	VW	W	W

<sup>a</sup>VW=very weak; W=weak; M=medium; S=strong; ?=ambiguous; N.D.=not detected.

<sup>b</sup>From crystal structure of **P3** in ref. 11c.

<sup>c</sup>Distance to pseudoatom between diastereotopic H nuclei.